JOURNAL OF CATALYSIS 151, 300–306 (1995)

On the Role of a $NiAl_2O_4$ Intermediate Layer in the Sintering Behavior of Ni/α-Al_2O_3

P. H. Bolt,*,† F. H. P. M. Habraken,* and J. W. Geus†

*Debye Institute, Department of Atomic and Interface Physics, Utrecht University, P.O. Box 80000, 3508 TA Utrecht, The Netherlands; and †Debye Institute, Department of Inorganic Chemistry, Utrecht University, P.O. Box 80083, 3508 TB Utrecht, The Netherlands

Received March 21, 1994; revised June 10, 1994

To investigate the reduction of $NiAl_2O_4$ and the sintering of Ni on α-Al_2O_3, Ni layers have been deposited onto polycrystalline α-Al_2O_3 substrates. Some samples were oxidized at 700°C and annealed at 1100°C in N_2/O_2 to convert the nickel layers completely into $NiAl_2O_4$. The reduction and sintering behavior of these layers was studied by Rutherford backscattering spectrometry, scanning electron microscopy, and X-ray diffraction. Temperature-programmed reduction showed that the onset temperature for the reduction of bulk $NiAl_2O_4$ is about 870°C. Due to the high temperatures required for the reduction of the $NiAl_2O_4/Al_2O_3$ samples, sintering of Ni during this treatment was inevitable. Our results indicate that there is a critical transition temperature for Ni sintering between 450 and 500°C. Nickel layers deposited onto $NiAl_2O_4/Al_2O_3$ samples showed exactly the same sintering behavior as Ni layers on bare α-Al_2O_3; thus, a continuous interfacial layer of $NiAl_2O_4$ does not inhibit sintering. However, substantially less sintering was observed for $Ni/NiAl_2O_4/Al_2O_3$ samples containing Ni particles on top of $NiAl_2O_4$ islands. A discontinuous interfacial $NiAl_2O_4$ layer is apparently required to slow the sintering of nickel on α-Al_2O_3.

INTRODUCTION

An important cause of catalyst deactivation is the formation of inactive compounds as a result of an extensive interaction between the active compound and its carrier. For example, Ni/Al_2O_3 catalysts can deactivate due to $NiAl_2O_4$ formation, especially at high temperatures (1–5). It is interesting to investigate whether the spent catalysts can be regenerated. Obviously, reduction of $NiAl_2O_4$ to Ni and Al_2O_3 by H_2 could provide a "fresh" Ni/Al_2O_3 catalyst, but it is doubtful whether such a regeneration treatment produces the desired small, highly dispersed nickel particles. Sintering of nickel, another cause of catalyst deactivation, may occur during reduction. Therefore, we investigated the reduction of $NiAl_2O_4$ and the sintering behavior of nickel on Al_2O_3 and on $NiAl_2O_4$.

The reducibility of bulk $NiAl_2O_4$ was compared to that of NiO by temperature-programmed reduction (TPR). Ni/α-Al_2O_3 samples were prepared by vapor deposition of Ni onto polycrystalline α-Al_2O_3 substrates. After oxidation to NiO, formation and reduction of $NiAl_2O_4$ were accomplished by annealing at high temperatures in N_2/O_2 and H_2, respectively. Subsequently, the samples were analyzed by Rutherford backscattering spectrometry (RBS) (6), X-ray diffraction (XRD), and scanning electron microscopy (SEM).

METHOD

Bulk nickel aluminate was prepared by calcining a 2 : 1 (mol/mol) mixture of $Al(NO_3)_3 \cdot 9H_2O$ and $Ni(NO_3)_2 \cdot 6H_2O$ (both supplied by Merck, Darmstadt, Germany) for 8 h at 1200°C. The purity of the $NiAl_2O_4$ was confirmed by XRD. Nickel oxide powder was supplied by Baker (Deventer, The Netherlands).

Polycrystalline α-Al_2O_3 substrates (7 × 12 mm; obtained from Gimex, Geldermalsen, The Netherlands, and from MRC (superstrate 996A), Orangeburg, NY) were cleaned from adhering organic impurities by rinsing with acetone and a subsequent heat treatment in air at 1200°C for 48 h. Nickel films (thickness about 80 nm) were vacuum vapor-deposited onto these substrates from an α-Al_2O_3 crucible, which was heated by a tungsten filament. The films were oxidized to NiO at 700°C in a flow of 80% N_2/20% O_2. Complete conversion of the NiO layers to $NiAl_2O_4$ was achieved by annealing the samples at 1100°C for 168 h. The completeness of the reaction has been confirmed by XRD, by RBS, and by the fact that the samples showed the characteristic light-blue color of $NiAl_2O_4$. Reduction treatments were performed in a flow of 100% H_2 at various temperatures and periods of time.

Temperature-programmed reduction was performed in a 50 ml/min 70% H_2/Ar flow at a heating rate of 5°C/min. Hydrogen consumption was detected by a hot wire detector (HWD). A cold trap containing dry ice retained the water produced.

RBS analysis was carried out with 2.868 or 2.008 MeV He^+ ions. The incident beam was parallel to the surface

0021-9517/95 $6.00

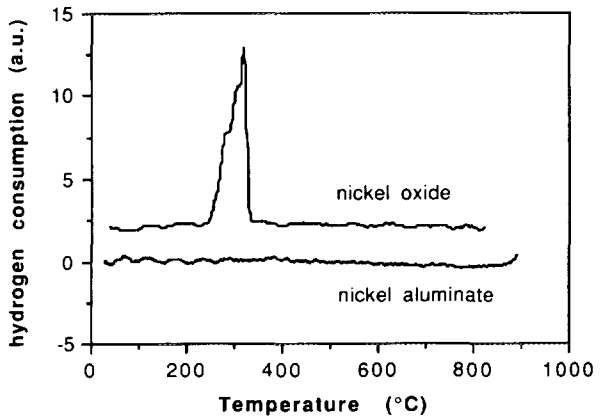

FIG. 1. TPR profiles of finely dispersed NiO and $NiAl_2O_4$ powder.

normal, and the detector was positioned at a scattering angle of 170°.

The X-ray diffractometer (Philips PW1140) was equipped with an Fe anode (λ = 1.9375 Å).

The lateral distribution of the nickel over the substrate was assessed with a Cambridge Stereoscan 150S scanning electron microscope equipped with detectors for secondary and backscattered electrons and with a Link AN 10000 X-ray analysis system with energy dispersive detector. The samples were mounted on an aluminum stub with carbon paste. A carbon layer was vacuum vapor-deposited onto the samples to provide a conducting surface.

RESULTS AND DISCUSSION

The TPR profiles of bulk nickel oxide and bulk nickel aluminate (Fig. 1) are totally different: Whereas the reduction of NiO starts well below 300°C and is completed rapidly, temperatures above 800°C are required to reduce $NiAl_2O_4$. This low reducibility of $NiAl_2O_4$ is a major reason that the formation of this compound in Ni/Al_2O_3 catalysts is highly undesirable.

To achieve the reduction of the $NiAl_2O_4$ layers at a sufficiently high reaction rate, $NiAl_2O_4/\alpha\text{-}Al_2O_3$ samples were annealed at 1000°C in H_2. The RBS results are shown in Fig. 2a, and the interpretation is presented in Fig. 2b. The solid and the dashed curves show the RBS spectra after deposition of the nickel and after subsequent complete reaction to $NiAl_2O_4$, respectively. As has been described before (5, 7), the nickel peak height decreases (due to dilution of the nickel atoms by Al and O) and the low energy edge shifts to lower energies (due to the penetration of nickel into the substrate) upon $NiAl_2O_4$ formation. At the same time, the aluminum edge moves to higher energies, indicating diffusion of Al^{3+} ions toward the surface.

When a $NiAl_2O_4/\alpha\text{-}Al_2O_3$ sample is treated at 1000°C in H_2 for 1 h, $NiAl_2O_4$ has been reduced to Ni. The sample turned black and in the X-ray diffractogram the Ni peaks at d = 2.03 and 1.76 Å are clearly visible. The $NiAl_2O_4$ peaks are no longer visible, so large $NiAl_2O_4$ crystallites are not present. In the RBS spectrum (dashed-dotted curve), the nickel peak height near the surface position has increased, a result which is caused by nickel enrichment at the surface. Obviously, the reduction treatment has resulted in nickel segregation toward the surface.

Upon prolonged treatment of the sample in H_2 at 1000°C, one might expect that complete segregation of nickel toward the surface would lead to a RBS spectrum similar to the spectrum of the "as-deposited" sample. This is definitely not the case. After 70 h at 1000°C in H_2, the RBS spectrum (dotted curve) shows that the surface concentration of nickel is even lower than that in the case of the unreduced $NiAl_2O_4/\alpha\text{-}Al_2O_3$ sample.

The explanation is provided by scanning electron microscopy. In the backscattered electron images (BEI, Fig. 3), large bright spots (diameter 1 μm) are visible on a dark background (Al_2O_3 substrate). Clearly, sintering of nickel has occurred, leaving a large fraction of the Al_2O_3 substrate uncovered and thus accounting for the low Ni/Al ratio at the surface shown in the RBS spectrum.

We thus have seen that upon annealing of $NiAl_2O_4/\alpha\text{-}Al_2O_3$ in H_2 at 1000°C, $NiAl_2O_4$ starts to reduce and metallic Ni segregates toward the surface. Prolonged treatment, however, leads to sintering of Ni. An interesting question arises: does the sintering start only after all the nickel aluminate has been reduced? Or, in other words, does an interfacial layer of $NiAl_2O_4$ prevent the sintering of nickel? We point out here that no nickel particles are visible in BEI after 1 h annealing at 1000°C in H_2.

To answer this question, a new series of $NiAl_2O_4/\alpha\text{-}Al_2O_3$ samples was prepared by vacuum vapor deposition of a thick Ni film (about 150 nm) onto polycrystalline $\alpha\text{-}Al_2O_3$ substrates. After oxidation to NiO the layers were annealed at 1100°C for 100 h to achieve complete conversion to $NiAl_2O_4$. Subsequently, another Ni layer (20 nm) was deposited onto these $NiAl_2O_4/\alpha\text{-}Al_2O_3$ samples and simultaneously onto bare $\alpha\text{-}Al_2O_3$ substrates. The $Ni/NiAl_2O_4/\alpha\text{-}Al_2O_3$ and $Ni/\alpha\text{-}Al_2O_3$ samples were kept simultaneously for 10 h at various temperatures in nonoxidizing (N_2 or H_2) atmospheres. If an interfacial layer of $NiAl_2O_4$ could inhibit sintering, the $Ni/NiAl_2O_4/\alpha\text{-}Al_2O_3$ samples would display much smaller nickel particles than the $Ni/\alpha\text{-}Al_2O_3$ samples.

In Figs. 4a and 4b, the relevant part of the RBS spectra of these samples and their interpretation, respectively, are shown. The spectra of both samples annealed at 450°C are identical to the corresponding spectra of unannealed samples; consequently no sintering occurs at 450°C. For the $Ni/\alpha\text{-}Al_2O_3$ sample (solid curve), only the nickel peak from the 20-nm Ni layer is shown. For the

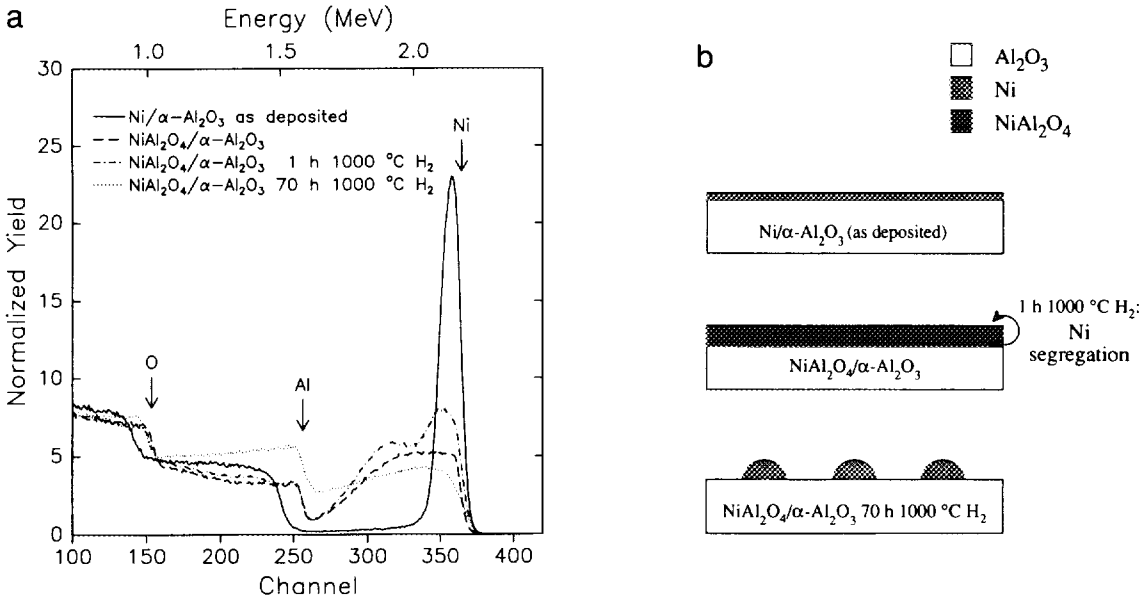

FIG. 2. (a) RBS spectra of $Ni/\alpha\text{-}Al_2O_3$ samples before and after complete reaction to $NiAl_2O_4$, and reduction for 1 and 70 h in H_2 at 1000°C. The arrows indicate the energy positions of surface scattering from the elements. The thickness of the nickel film amounts to about 80 nm. Beam: 2.868 MeV He^+. (b) Interpretation of (a). The schematic drawings correspond to the RBS spectra of (a).

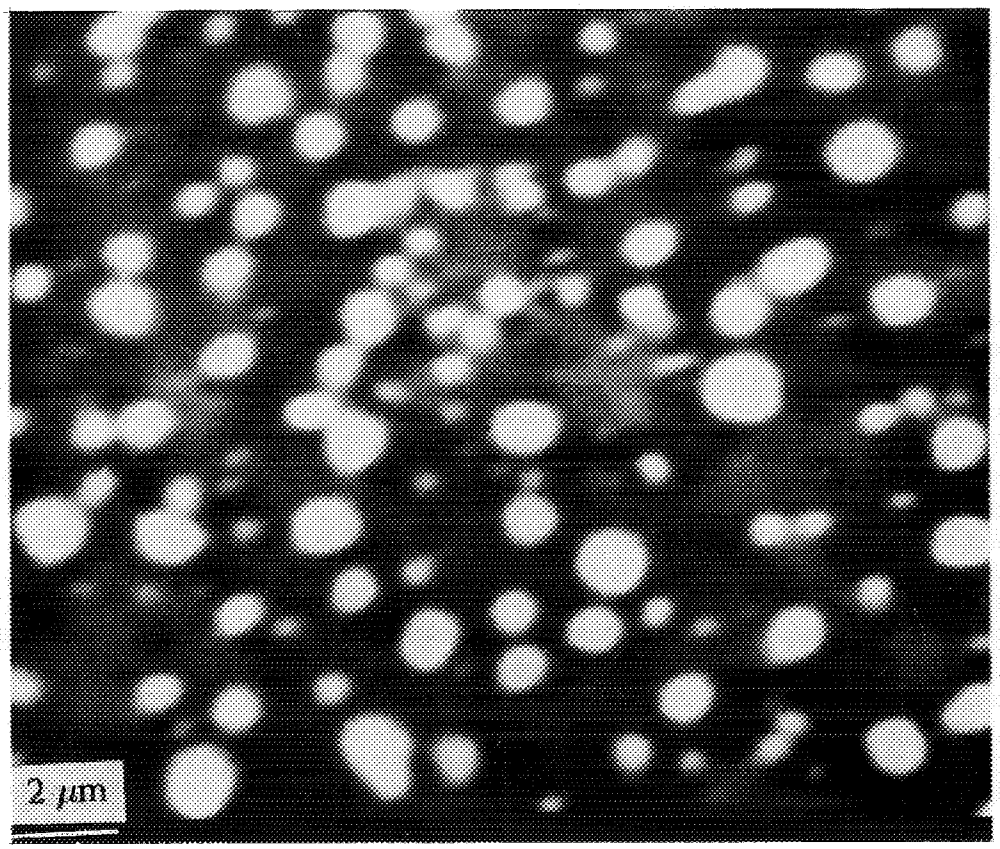

FIG. 3. Back-scattered electron image of $NiAl_2O_4/\alpha\text{-}Al_2O_3$ after 70 h at 1000°C in H_2.

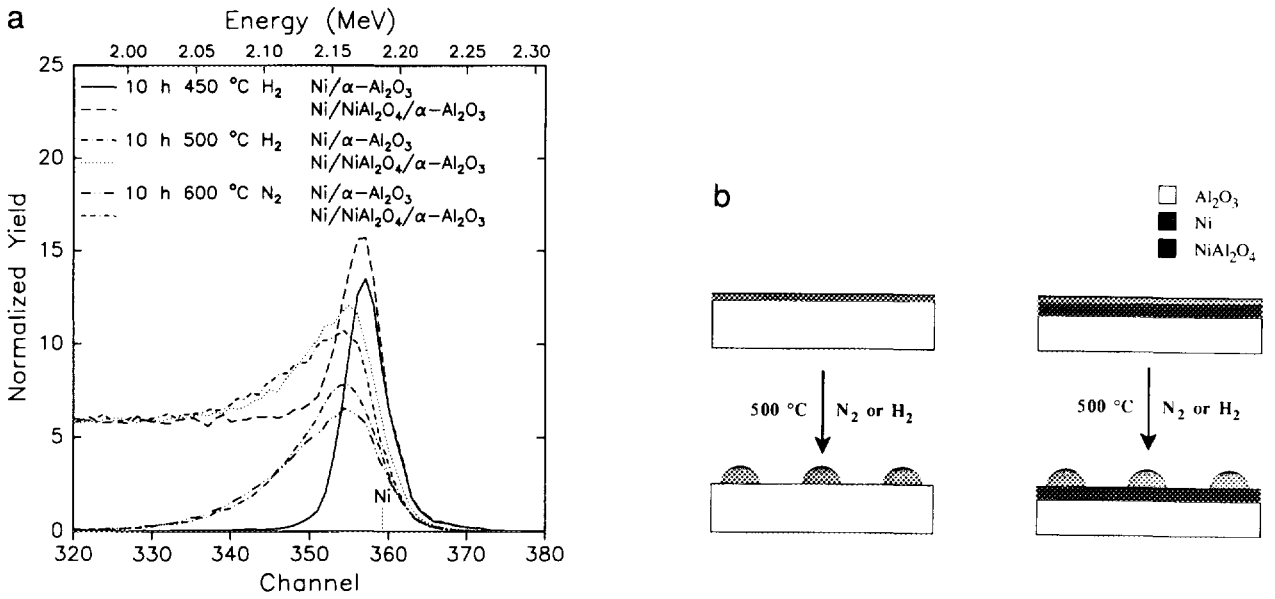

FIG. 4. (a) RBS spectra of Ni/α-Al_2O_3 and $Ni/NiAl_2O_4/\alpha$-Al_2O_3 samples after annealing for 10 h at 450, 500, and 600°C in H_2 or N_2. The thickness of the nickel film amounts to about 20 nm. Beam: 2.868 MeV He^+. (b) Schematic overview of experiments and results concerning the influence of a continuous interfacial $NiAl_2O_4$ layer on the sintering of Ni on α-Al_2O_3. The drawings correspond to the RBS spectra of (a).

$Ni/NiAl_2O_4/\alpha$-Al_2O_3 sample, the same peak is visible, superimposed on the signal originating from the thick $NiAl_2O_4$ layer, which is responsible for the constant level at the low-energy side. After annealing at 500°C, the nickel peak height of both the Ni/α-Al_2O_3 and the $Ni/NiAl_2O_4/\alpha$-Al_2O_3 sample has decreased markedly, and a tail at the low-energy side has evolved. The shapes of the tails are similar in both spectra. Apparently, there is no difference between the two sample types with respect to the sintering behavior of the nickel. Furthermore, the change of the profile of the nickel peaks indicates that there is a critical transition temperature between 450 and 500°C for the sintering of supported nickel. It is noteworthy that this temperature is significantly above the Hüttig temperature (about 1/3 T_m, i.e., 575 K or 302°C; T_m = melting point (K)), the onset of surface diffusion (8), and below the Tammann temperature (about 0.5 T_m, i.e., 863 K or 590°C) where bulk diffusion commences (9). The results are in agreement with those of a study on Ni/Al_2O_3 catalysts in which sintering of the Ni particles is observed at 530°C (10).

Annealing ay 600°C leads to some additional sintering, which is evidenced by a further decrease in nickel peak height in the RBS spectra and tails which extend slightly further.

SEM confirmed that the sintering behavior of the Ni/α-Al_2O_3 and the $Ni/NiAl_2O_4/\alpha$-Al_2O_3 samples is essentially the same. In BEI (Fig. 5) bright spots of the same mean size originating from Ni particles are visible for both samples annealed at 600°C for 10 h. The contrast in the BEI photograph of $Ni/NiAl_2O_4/\alpha$-Al_2O_3 (Fig. 5b) is less sharp because of a more intense background signal, due to the presence of the $NiAl_2O_4$ layer.

As is schematically summarized in Fig. 4b, we have seen that a continuous interfacial layer of $NiAl_2O_4$ does not inhibit the sintering of nickel on α-Al_2O_3. This conclusion is surprising since it is generally assumed that a good interaction between the active component of a catalyst and its support might slow the sintering of the former. An interfacial nickel aluminate layer is supposed to provide such a good interaction in the case of Ni/Al_2O_3 catalysts. As a next step we investigated whether a discontinuous $NiAl_2O_4$ layer prevents sintering.

To this end, a series of Ni/α-Al_2O_3 samples (deposited Ni layer, 70 nm) was annealed in H_2 at 550°C for 20 h to allow the Ni to sinter slightly (step A). Subsequently, some of these samples were kept at 1000°C in O_2 for 12 h (step B). In this treatment nickel is oxidized to NiO and the interfacial reaction between NiO and α-Al_2O_3 to $NiAl_2O_4$ proceeds, but only to a very limited extent. Because of the sintering prior to this treatment, the $NiAl_2O_4$ layer will be discontinuous. Finally, such $NiO/NiAl_2O_4/\alpha$-Al_2O_3 samples were kept in H_2 for 12 h at 650 or 750°C (step C), simultaneously with Ni/α-Al_2O_3 samples which had undergone step A but not step B. During this treatment, NiO is rapidly reduced to Ni, but $NiAl_2O_4$ remains unreduced.

In Fig. 6a RBS spectra, measured after the various sample treatments, are shown. Figure 6b demonstrates our interpretation of these results. The solid curve in Fig.

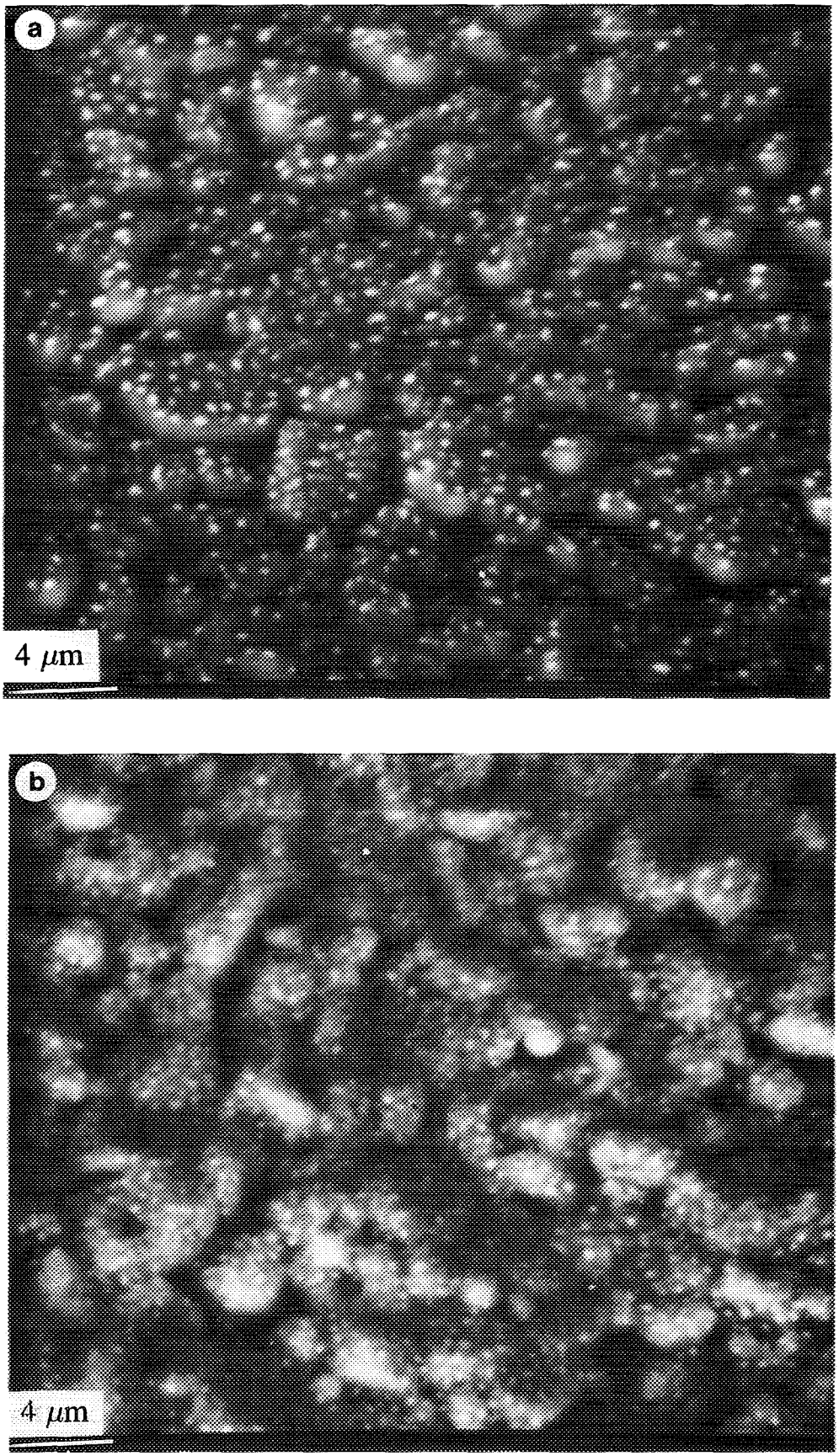

FIG. 5. BEI micrographs of (a) Ni/α-Al_2O_3 and (b) Ni/$NiAl_2O_4$/α-Al_2O_3 samples after 10 h at 600°C in a flow of N_2.

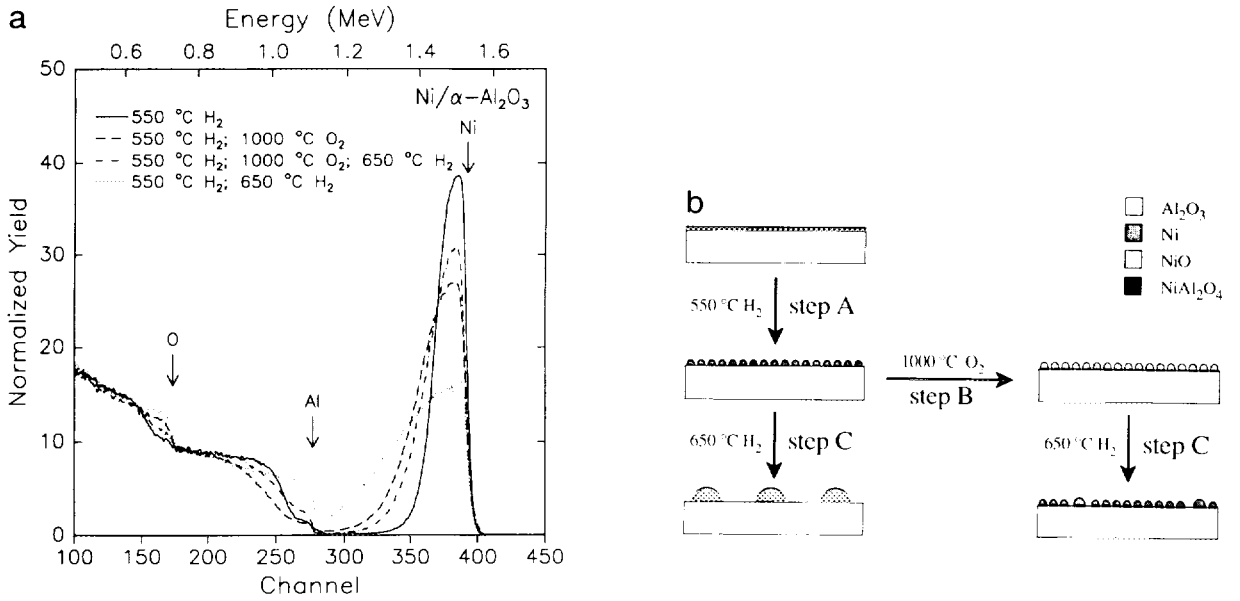

FIG. 6. (a) RBS spectra of Ni/α-Al_2O_3 samples after annealing for 20 h at 550°C in H_2 (step A), after step A and subsequent annealing for 12 h at 1000°C in O_2 (step B), after step A and step B and subsequent annealing for 12 h at 650°C in H_2 (step C), and after step A and step C without step B. The thickness of the nickel film amounts to about 70 nm. Beam: 2.008 MeV He^+. (b) Schematic overview of experiments and results concerning the influence of a discontinuous interfacial $NiAl_2O_4$ layer on the sintering of Ni on α-Al_2O_3. The drawings correspond to the RBS spectra of (a).

6a represents the spectrum after step A. From the shape of the Al and O edges it is apparent that some uncovered Al_2O_3 is already present. In step B (dashed curve) the nickel is oxidized and thus the nickel atoms are diluted with oxygen atoms. Therefore, the nickel peak becomes lower and broader, the oxygen edge rises, and the low-energy side of the stepped aluminum edge shifts to lower energies. From this last observation it becomes clear that during step B there is hardly any additional sintering, and the interfacial aluminate formation is indeed very limited. The high-energy side of the aluminium edge, however, remains at the surface energy position, which means that some fraction of the Al_2O_3 substrate is still uncovered.

After all three steps (dashed-dotted curve; step C at 650°C) the NiO is reduced again to Ni. The nickel peak becomes higher than after step B (because of the removal of the diluting oxygen atoms), but not as high as after step A, which means that some additional sintering has occurred. The fact that the shapes of the aluminum and oxygen edges indicate an increased fraction of uncovered Al_2O_3 is in agreement with this observation.

Remarkably different, however, is the RBS spectrum (dotted curve) of the sample that has been subjected to step A and step C (at 650°C) but not to step B. It is obvious from the low, broad nickel peak and the high aluminum and oxygen edges at the surface energy positions that severe sintering has taken place, which is confirmed by SEM. The fraction of uncovered Al_2O_3 has risen from 30% after step A to 79% after the combined step A and step C at 650°C (Table 1). The intermediate step B leading to a discontinuous interfacial layer limits this amount to 42%. Similar results have been obtained when step C is performed at 750°C. From Table 1 it is apparent that the effect of the ommission of step B is larger than the effect of a 100°C temperature increase during step C.

The above results, which are schematically summarized in Fig. 6b, show clearly that a discontinuous interfacial layer of $NiAl_2O_4$ slows the sintering of nickel on alumina. A continuous nickel aluminate layer, however, has no effect on the sintering rate of Ni. Analogous behavior has been reported for $Ag/SnO_2/\alpha$-Al_2O_3 catalysts; the interfa-

TABLE 1

Extent of Sintering of Ni, Calculated from the RBS Spectra

Sample treatment[a]	Fraction of Al_2O_3 in near-surface region (%)
A	30
A + B	20
A + B + C650	42
A + C650	79
C650	50
A + B + C750	63
A + C750	83

[a] A, 20 h at 550°C in H_2; B, 12 h at 1000°C in O_2; C650, 12 h at 650°C in H_2; and C750, 12 h at 750°C in H_2.

cial SnO_2 layer must be discontinuous to prevent the sintering of Ag (11).

A possible explanation can be found in interfacial energy considerations. Rather than the absolute value of the interfacial energy, the variations in the interfacial energy with the position on the surface of the metallic nickel particles determine the surface mobility of the metal particles. Though $NiAl_2O_4$ will bind metallic nickel particles more strongly, the variations in binding energy with the position on the surface are likely to be small. The experimental results indicate that the variations in binding energy are of the same order of magnitude as those with α-Al_2O_3. With a discontinuous layer of $NiAl_2O_4$, however, the difference in binding energy on $NiAl_2O_4$ and α-Al_2O_3 anchors the metallic nickel particles to the $NiAl_2O_4$ patches.

One might argue that the experimentally observed results could also be explained by redispersion of nickel during step B. Ruckenstein and Lee (10) studied the redispersion and sintering of Ni/Al_2O_3 by transmission electron microscopy. They observed that nickel particles, when oxidized to NiO, spread over the substrate to a lower wetting angle. Crystallites larger than about 175 Å changed their shape from circular to toroidal. A subsequent short reduction treatment (1 h at 530°C in H_2) led to the splitting of the torus due to contraction of the interlinked units of the torus to a greater wetting angle. This resulted in considerable redispersion of the nickel. Subsequent prolonged heating in H_2 caused sintering of the Ni.

In step B, the Ni crystallites in the samples are also oxidized to NiO, and this might cause some redispersion of Ni. However, this could not sufficiently account for the observed large difference in sintering behavior between the Ni/α-Al_2O_3 and the $Ni/NiAl_2O_4/\alpha$-Al_2O_3 samples. Table 1 shows some decrease (from 30 to 20%) of the Al_2O_3 fraction in the near-surface region, but this could also be attributed to the volume increase of the nickel particles during oxidation. Redispersion effects will be small, much smaller than in the study mentioned above (where the total amount of nickel per cm^2 of Al_2O_3 and the reduction temperature were considerably lower), and rather rapidly cancelled out during step C. Moreover, a larger fraction of uncovered Al_2O_3 is found (50%) and thus more sintering of Ni has occurred after step C at 650°C even without step A compared to the corresponding sample subjected to all three steps (42%). Therefore, the explanation for the observed reduction of nickel sintering appears to be consistent with the anchoring of Ni by a discontinuous aluminate layer.

CONCLUSIONS

A discontinuous interfacial layer of $NiAl_2O_4$ slows the sintering of nickel on α-Al_2O_3, but a continuous layer has no effect.

No sintering of nickel on α-Al_2O_3 has been observed at 450°C, but substantial sintering occurred at 500°C. Apparently, there is some critical transition temperature between 450 and 500°C for the sintering of nickel on α-Al_2O_3.

Because of the high onset temperature for the reduction of $NiAl_2O_4$ (about 870°C, more than 600°C higher than that for NiO), sintering of nickel is inevitable during the reduction of Ni/Al_2O_3 catalysts which have been deactivated by $NiAl_2O_4$ spinel formation. Therefore, such a treatment will not lead to a fully regenerated catalyst. This will be true even for catalysts still containing some Ni which has not reacted to spinel; the presence of such nickel species may lead to a lowering of the $NiAl_2O_4$ reduction onset temperature due to hydrogen spillover.

ACKNOWLEDGMENTS

The authors thank the crew of the accelerator department of Utrecht University for running the accelerator, and Miss F. van Looij for operating the scanning electron microscope. This work has been supported by the Stichting Scheikundig Onderzoek Nederland (SON).

REFERENCES

1. Delmon, B., and Grange, P., *in* "Progress in Catalyst Deactivation: Proceedings of the NATO Advanced Study Institute on Catalyst Deactivation" (J. L. Figueiredo, Ed.), p. 231. Martinus Nijhoff Publishers, The Hague, 1981.
2. Chernavskii, P. A., and Lunin, V. V., *Kinet. Catal.* **34,** 470 (1993).
3. Lo Jacono, M., Schiavello, M., and Cimino, A., *J. Phys. Chem.* **75,** 1044 (1971).
4. Gavalas, G. R., Phichitkul, P., and Voecks, G. E., *J. Catal.* **88,** 54 (1984).
5. Bolt, P. H., Lobner, S. F., van den Bout, T. P., Geus, J. W., and Habraken, F. H. P. M., *Appl. Surf. Sci.* **70/71,** 196 (1993).
6. Chu, W.-K., Mayer, J. W., and Nicolet, M.-A., "Backscattering Spectrometry." Academic Press, New York, 1978.
7. De Roos, G., De Wit, J. H. W., Fluit, J. M., Geus, J. W., and Velthuizen, R. P., *Surf. Interface Anal.* **5,** 119 (1983).
8. Spencer, M. S., *Nature* **323,** 685 (1986).
9. Dowden, D. A., *in* "Progress in Catalyst Deactivation: Proceedings of the NATO Advanced Study Institute on Catalyst Deactivation" (J. L. Figueiredo, Ed.), p. 281. Nijhoff, The Hague, 1981.
10. Ruckenstein, E., and Lee, S. H., *J. Catal.* **86,** 457 (1984).
11. Meima, G. R., van Leur, M. G. J., van Dillen, A. J., Geus, J. W., Boogaarts, J. E., van Buren, F. R., Derks, L. J. G. M., and Delcour, K., *Appl. Catal.* **44,** 133 (1988).